Relationship between Streaming Potential and Compressive Stress in Bovine Intervertebral Tissue

Kazuhiro Fujisaki[1], Shigeru Tadano[1], Nozomu Asano[1]

1 Division of Human Mechanical Systems and Design, Faculty of Engineering,

Hokkaido University, Kita-13, Nishi-8, Kita-ku, Sapporo 060-8628, Japan

Corresponding author: Kazuhiro Fujisaki

Division of Human Mechanical Systems and Design, Faculty of Engineering,

Hokkaido University, Kita-13, Nishi-8, Kita-ku, Sapporo 060-8628, Japan

Tel. & Fax: +81-11-706-6396

E-mail: fujiwax@eng.hokudai.ac.jp

Manuscript type: Original Articles

Running title: Streaming Potential in Bovine Intervertebral Tissue

Abstract

The intervertebral disc is formed by the nucleus pulposus (NP) and annulus fibrosus (AF), and intervertebral tissue contains a large amount of negatively charged proteoglycan. When this tissue becomes deformed, a streaming potential is induced by liquid flow with positive ions. The anisotropic property of the AF tissue is caused by the structural anisotropy of the solid phase and the liquid phase flowing into the tissue with the streaming potential. This study investigated the relationship between the streaming potential and applied stress in bovine intervertebral tissue while focusing on the anisotropy and loading location. Column-shaped specimens, 5.5 mm in diameter and 3 mm thick, were prepared from tissue of the AF, NP, and the annulus-nucleus transition region (AN). The loading direction of each specimen was oriented in the spinal axial direction, as well as in the circumferential and radial directions of the spine considering the anisotropic properties of the AF tissue. The streaming potential changed linearly with stress in all specimens. The linear coefficients k_e of the relationship between stress and streaming potential depended on the extracted positions. These coefficients were not affected by the anisotropy of the AF tissue. In addition, these coefficients were lower in AF than in NP specimens. Except in the NP specimen, the k_e values were higher under faster compression rate conditions. In cyclic compression loading, the streaming potential changed linearly with compressive stress, regardless of differences in the tissue and load frequency.

Key words:

Biomechanics, Streaming potential, Intervertebral tissue, Uniaxial loading, Viscoelastic property

1. Introduction

The spine is formed by a series of vertebrae and intervertebral discs in addition to muscles and ligaments. The biological function of the intervertebral discs is to provide motion flexibility and stiffness to support the body weight. Intervertebral disc tissue is classified into either nucleus pulposus (NP) or annulus fibrosus (AF). NP is located in the center of the tissue and surrounded by a layer forming the AF. The AF contains numerous collagen fibers that are composed of concentric layers encircling the NP. The collagen fibers are oriented in layers that intersect with each other (White and Panjabi, 1978). Urban and Maroudas (1979) stated that the NP contains much more liquid than the AF. Understanding the interplay between applied stress in human motion for a variety of situations and body weights is important to the analysis of injuries of this tissue. Many types of stress/strain analyses of the spine have been carried out to explain the mechanical properties of biological soft tissue, and a number of physical models have been proposed in analytical studies. In these models, the properties are described on the basis of their approximate elasticity or viscoelasticity (Bilston and Thibault, 1996, Ichihara et al., 2003). In addition, there are biphasic models that consider the interaction of the solid and liquid phases (Ateshian et al., 1997, LeRoux and Setton, 2002, Perie et al., 2004). When the phases become deformed, the liquid phase in the tissue flows out through openings in the solid phase, and the interaction and friction between the two phases give rise to macroscopic viscoelastic behavior. In addition, the solid phase of soft tissue contains a large amount of negatively charged proteoglycan, which is caused by glycosaminoglycan having negatively charged sulfate and carboxyl groups. Strain in the soft tissue changes the charge density of the proteoglycan and disrupts the balance of the electrochemical equilibrium. This electrical charge affects

the viscoelastic deformation of the tissue. The triphasic theory was proposed to describe the mechanical properties of articular cartilage (Lai et al., 1991, Gu et al., 1993, Lai et al., 2000, Ateshian et al., 2004, Sun et al., 2004) while considering the solid and the liquid phases as well as the negative ion phase. When an electrical potential is present in the deformed tissue, the potential changes with the liquid flow. This relative change in electrical potential is referred to as the streaming potential. The streaming potential has been measured in articular cartilage (Frank et al., 1987a, 1987b, Chen et al., 1997, Garon et al., 2001), lumbar discs (Gu et al., 1999), tendons (Chen et al, 2000), spinal cords (Tadano et al., 2009), and bone (Gross and Williams, 1982). The triphasic theory postulates that stress causes streaming potential. It has also been reported that the relationship between stress and electrical potential of the spinal cord tissue is linear in uniaxial compressive loading (Tadano et al., 2009). Knowledge of the streaming potential would enable stress measurements of the viscoelastic tissue. The fiber-oriented structure characterizes the anisotropic elasticity of the tissue, and stress estimates of the tissue should be analyzed by considering the anisotropic elastic modulus of the AF tissue. This study was conducted to investigate the relationship between the anisotropic structure of the AF and the streaming potential generated by a range of compressive loads applied from different directions. The streaming potentials in the AF tissue were then compared with those in the NP tissue under the same compressive loading conditions.

2. Experimental Procedure

2.1 Measurement of streaming potential

Quantitative measurements of the streaming potential related to tissue compression can be performed using uniaxial compression under a condition in which there is unidirectional inner liquid flow, and a confined compression testing device has been constructed to measure streaming potential with unidirectional flow (Tadano et al., 2009). Figure 1 shows the test setup based on a commercially available material testing machine (Instron Model 3365, Instron Corp., with 50 N load cell). This setup was primarily used for compressive tests in conjunction with an indenter. In the present study, a porous 6-mm-thick plastic plate (Fildus S-HP6.0, Mitsubishi Plastics, Inc.) was used as the filter for the liquid phase flowing from the specimen under strain. This plate was made from small particles (125 μm in diameter) of ultrahigh-molecular-weight polyethylene and had a porosity of 52 vol%. The porous filter prevents outflow of the solid phase but does not obstruct inflow or outflow of the liquid phase. In this system, the specimen is placed in a 5.5-mm inner diameter acrylic ring that is set on the porous filter. The ring restrains the circumference of the specimen, and the internal liquid phase only moves to the filter side to flow out through the porous filter during compression loads applied from above. Differences in the electrical potential then arise in the specimen because the negatively charged proteoglycan in the solid phase remains and is concentrated in the compressive area of the specimen, while the positive ions flow through the tissue. In this study, the assembled structure was set inside a clear acrylic container filled with physiological saline. The container was located in a large bath and kept at 37 °C by supplying hot water to the surrounding bath. An Ag/AgCl electrode (E204 Disk, IMV Corp.) bonded and insulated from the tip of the 5-mm diameter indenter was used to test the physiological conditions. This type of electrode is useful under these conditions because it does not dissolve in solutions

containing chlorine ions and hence prevents damage to biological specimens during measurements. Another electrode used as a reference electrode was located in the physiological saline bath 30 mm from the loading axis at the same height as the specimen to avoid the effects of liquid phase flow out (Fig. 1). The electrical potential between these two electrodes was measured as the streaming potential focused on the loading location. The electrical potential is detected by electrodes using an amplifying device (CDV-700A, Kyowa Electric Instruments Co. Ltd.). The potential is recorded on a PC by a sensor interface (PCD-300A, Kyowa Electric Instruments Co. Ltd.) concurrently with the applied load at the indenter measured from the load cell. Overall, the system measures electrical potential changes in the tissue specimen during compressive loading.

2.2 Specimens

Intervertebral discs were removed from the lumbar spine of three female 24-month-old Holstein cows that had died for reasons other than spine diseases. The lumbar disc tissue was then extracted from the spine and preserved at less than 5 °C for less than three days after death, after which the discs were preserved by freezing at -35 °C. Figure 2(a) shows a photograph of a cross section of an intervertebral disc, and Fig. 2(b) shows the locations at which the specimen was cut. Column-shaped specimens that were 3 mm thick and had a diameter of 5.5 mm were prepared from the lumbar discs. The loading direction of each specimen was oriented in the spinal axial direction in the NP and the AN (annulus-nucleus transition region) specimens, as shown in Fig. 2(b). In the AF specimens, the axial (AF-A), circumferential (AF-C), and radial

directions (AF-R) of the spine were sampled for measurement of the anisotropic elasticity of the AF tissue. Nine specimens of each tissue type were prepared from several parts of the lumbar discs in the three cows, and the mean value of the nine specimens was determined and used for subsequent analysis. The specimens were cryogenically preserved in a freezer at -35 °C until immediately before the loading experiments. Compression specimens, 5.5 mm in diameter and 3 mm thick, were formed using a punch cutter while the specimens were frozen. When the frozen specimens were thawed after being set in the testing device and placed in physiological saline at a constant temperature of 37 °C, their height changed considerably owing to swelling. To prevent resistant forces from arising in the loading tests as a result of swelling, a sufficient interval of more than 35 min was maintained between placement in the saline and the beginning of the tests. However, the volume of swelling varied among specimens, and the thicknesses of specimens during swelling could not be kept constant. Therefore, the indenter was placed 4 mm above the surface of the bottom filter after the specimen was set, as shown in Fig. 3. The inner container was filled with physiological saline and the temperature was kept constant by the surrounding water (37 °C) during the experiments. All specimen heights were kept at 4 mm after sufficient swelling from the 3 mm frozen height, and the stress, strain, and electrical potential were set to zero as the initial values.

2.3 Loading patterns

Compression loading and long period loading by cyclic loads were carried out to relate the streaming potential to a variety of stress states. The compression loading

profile is shown in Fig. 4. Three phases of the compression process, 8.0 mm/min for 3 s, 0.8 mm/min for 15 s, and 0.08 mm/min for 150 s, resulting in a 0.4, 0.2, and 0.2 mm compression, respectively, with a total of 0.8 mm of compression, were carried out under the wet condition with the physiological saline at 37 ± 1 °C. After the compression processes, cyclic compression loads with a constant frequency of either 0.01, 0.1, or 1 Hz and total amplitude of 0.2 mm were applied to the specimen during 30 min. When the loading conditions were changed, time intervals of 35 min were used to maintain the stability of the specimens and release both stress and electrical potential close to the initial values.

3. Results

3.1 Monotonic compression test

The electrical potential between the electrode attached to the tip of the indenter and the reference electrode became increasingly negative as the applied compressive strain increased. Figure 5(a) shows the stress and strain curves calculated from the applied load in the AF specimens under uniaxial compression at a compression rate of 0.8 mm/min. Figure 5(b) shows the relationships between the electrical potential and strain in the AF specimens under the same conditions as those in Fig. 5(a). The results indicate a non-linear relationship between the stress and strain, as well as between the steaming potential and the strain. Figure 5(c) shows the relationship between the streaming potential V and the compressive stress σ. This relationship was linear and had a very high correlation coefficient R^2 of more than 0.99 for every specimen. This linear relationship is expressed in Eq. (1).

$$V = k_e \sigma \quad (1)$$

where k_e is the electrokinetics factor. As shown in Fig. 6, the mean values of k_e (n = 9) measured for each specimen at different compression rates varied depending on the extraction location and compression speed. The difference of each mean value of k_e was evaluated in two sample *t*-test. In the case of un-equal variances, Welch's *t*-test was used to evaluate the difference. The results showed that there were no significant differences in k_e among loading directions -A, -C, and -R in the AF specimens at each of the loading speeds. Significant differences in k_e were observed between each AF specimen and the NP specimen, under compression at 0.08 mm/min ($p < 0.01$) and 0.8 mm/min ($p < 0.05$). In the NP specimens, the k_e values for the different compression speeds were very similar, but these values varied greatly among specimens. The k_e values were higher for higher compression speeds in AF-A ($p < 0.01$) and AF-C ($p < 0.01$), while the k_e values of the AF-R and AN specimens did not differ significantly.

3.2 Cyclic loading test

Figure 7 shows the relationship between the compressive stress and streaming potential for the entire 30-min period of cyclic loading at 0.01 Hz in AF-A. A linear relationship was observed for all specimens. The response of the electric charge showed no time delay and the measured electrical potential pattern had negative peaks at the maximum compression stress in the loading. The amplitude of the peak-to-peak streaming potential for all specimens decreased slightly as the cycle number increased. The k_e values were calculated in the same manner as in the case of the compression curves, i.e., as an average value of the entire cyclic loading period. The values could be

regarded as independent of the cyclic frequency after the second loading among the same types of specimens (data not shown). Figure 8 shows the mean values of k_e in each specimen (n = 9) averaged for all cyclic speeds. The effects of the anisotropic structure of the AF were not apparent in these results. Although there were no apparent differences in the tissue, the NP specimens showed higher k_e values than the AF specimens, similar to the results of the uniaxial compression experiments. Although the AN values varied greatly, their values were between those of AF and NP.

4. Discussion

The system developed here provides the streaming potential generated in the soft tissue under compressive conditions while considering a specific stress field. The experiments consisted of *in vitro* tests performed outside of the biological body, and the streaming potential was determined based on the electrical difference between the loading area and the outside of the specimen during compressive loading in physiological saline. Compression deformation was concentrated at the vicinity of the indenter and then transferred to the bottom side of the specimen via liquid flow during the tissue deformation. Because the measurement system detects electrical changes using an electrode attached at the indenter, the streaming potential was obtained based on dynamic changes in the localized stress field.

The specimens were kept in physiological saline at 37 °C to maintain an environment close to the *in vivo* conditions. However, the specimens were frozen at -35 °C before the tests to form the column shape and to preserve the samples. Some structural damage such as disconnects in the microscopic fiber structures and

disappearance of proteoglycan may have occurred during the swelling process. Such changes would have affected the relationships between the stress and strain, as well as between the stress and streaming potential, as the overall environment was different from the *in vivo* conditions. The stresses in the disc tissue were highly dependent on the liquid phase outflow under this strain condition. If there is a change in stress in the disc tissue in actual situations, liquid flow occurs, resulting in changes in the electrical potential. Therefore, measurements of changes in the electrical potential offer an avenue to investigate the stress and strain of intervertebral discs under *in vivo* conditions. Berkenblit et al. (1994) proposed that techniques for detection of the electrokinetic properties were useful for nondestructive measurement of osteoarthritis. Quenneville et al. (2004) developed a microelectrode array device for the detection of the streaming potential during diagnosis of the state of cartilage. These studies indicated that load-bearing tissue such as cartilage and discs could be evaluated using streaming potential measurements.

Although anisotropic properties were evident in AF-A and AF-C, and AF-A and AF-R specimens (Fig. 5(a)), the linear relationships between the stress and the streaming potential k_e showed almost no differences among these specimens under the same loading speed, as shown in Fig. 6. Reynaud and Quinn (2006a) investigated the hydraulic permeability of the cow's proximal articular surfaces and found that the electrokinetic properties exhibited isotropic phenomena, regardless of the loading directions in the anisotropic matrix; therefore, these properties could be regarded as a robust indicator for evaluating the clinical conditions of the tissue (Reynaud and Quinn, 2006b). These findings suggest that the relationship can be used under stress conditions as a direct method of measurement without other structural observations involving

anisotropy. The k_e values were lower in the AF specimens than in the NP specimens, which is consistent with the amounts of negatively charged glucosaminoglycan in proteoglycan. Urban and Maroudas (1979) and Iatridis et al. (2009) showed that the glucosaminoglycan content was higher in the central region, with the highest values being observed at the NP of intervertebral discs. The streaming potential depends on the movement of positive ions in the fluid flow, and the k_e values change with the compression speed. In the present study, the values were higher for higher compression rates in almost all specimens, except in the NP specimens. The proteoglycan rich tissue may exhibit low permeability because the liquid phase is composed of polar molecules and therefore has a higher flow resistance through solid matrices with negatively charged proteoglycan (Mansour and Mow, 1976). Although the speed of the flow increased as the compression rates increased, even in the NP specimens, the friction between the liquid and the solid phases also increased, resulting in higher stress conditions. Therefore, k_e may have smaller values with high stress at the same compression rates when compared with the other tissue samples.

Linear relationships between the stress and electrical potential generated were obtained under both the monotonic compression and stress release processes in the cyclic loadings. Such a linear relationship has also been observed during measurement of cartilage specimens under compression and creep conditions (Chen et al., 1997). The compression rate and initial thickness were changed in the uniaxial compression experiments. The stress-streaming potential relationships were linear with a constant coefficient k_e during each loading period, and k_e was lower at lower compression rates. In the cyclic loading, the linear coefficients k_e were very similar, regardless of frequency changes. The differences between the monotonic compression and the cyclic

loading could be considered as the stress and electrical potential relaxation, which were dependent on the deformation speed. The continuous loading and unloading process might have prevented sufficient stress and electric relaxation, even under lower loading speeds at 0.01 Hz. The stress and electrical potential were almost completely released after 35 min of relaxation after compression. This is similar to the results reported in an analytical study of stress relaxation under compression of articular cartilage based on the triphasic theory (Lai et al., 2000). Therefore, it can be concluded that the streaming potential is related to the viscoelastic properties of both the AF and NP tissues in triphasic studies.

Conflict of Interest Statement

The authors have no actual or potential conflicts of interest to declare.

References

Ateshian, G. A., Warden, W. H., Kim, J. J., Grelsamer, R. P., Mow, V. C., 1997. Finite deformation biphasic material properties of bovine articular cartilage from confined compression experiments, Journal of Biomechanics 30, 1157-1164.

Ateshian, G. A., Chahine, N. O., Basalo, I. M., Hung, C. T., 2004. The correspondence between equilibrium biphasic and triphasic material properties in mixture models of articular cartilage, Journal of Biomechanics 37, 391-400.

Berkenblit, S. I., Frank, E. H., Salant E. P., Grodzinsky, A. J., 1994. Nondestructive detection of cartilage degeneration using electromechanical surface spectroscopy,

Journal of Biomechanical Engineering 116, 384-392.

Bilston, L. E., Thibault, L. E., 1996. The mechanical properties of the human cervical spinal cord in vitro, Annals of Biomedical Engineering 24, 67-74.

Chen, A. C., Nguyen, T. T., Sah, R. L., 1997. Streaming potentials during the confined compression creep test of normal and proteoglycan-depleted cartilage, Annals of Biomedical Engineering, Biomedical Engineering Society 25, 269-277.

Chen, C., McCabe, R. P., Grodzinsky, A. J., Vanderby Jr., R., 2000. Transient and cyclic responses of strain-generated potential in rabbit patellar tendon are frequency and pH dependent, Journal of Biomechanical Engineering 122, 465-470.

Frank, E. H., Grodzinsky, A. J., Koob, T. J., Eyre, D. R., 1987a. Streaming potentials: a sensitive index of enzymatic degradation in articular cartilage, Journal of Orthopaedic Research 5, 497-508.

Frank, E. H., Grodzinsky, A. J., 1987b. Cartilage Electromechanics-I. Electrokinetic transduction and the effects of electrolyte pH and ionic strength, Journal of Biomechanics, 20, 615-627.

Garon, M., Legare, A., Guardo, R., Savard, P., Buschmann, M. D., 2001. Streaming potentials maps are spatially resolved indicators of amplitude, frequency and ionic strength dependent responses of articular cartilage to load, Journal of Biomechanics 35, 207-216.

Gross, D., Williams, W. S., 1982. Streaming potential and the electromechanical response of physiologically-moist bone, Journal of Biomechanics 15, 277-295.

Gu, W. Y., Lai, W. M., Mow, V. C., 1993. Transport of fluid and ions through a porous-permeable charged-hydrated tissue, and streaming potential date on normal bovine articular cartilage, Journal of Biomechanics 26, 709-723.

Gu, W. Y., Mao, X. G., Rawlins, B. A., Iatridis, J. C., Foster, R. J., Sun, D. N., Weidenbaum, M., Mow, V. C., 1999. Streaming potential of human lumbar anulus fibrosus is anisotropic and affected by disc degeneration, Journal of Biomechanics 32, 1177-1182.

Iatridis, J. C., Furukawa, M., Stokes, I. A. F., Gardner-Morse, M. G., Laible, J. P., 2009. Spatially resolved streaming potentials of human intervertebral disk motion segments under dynamic axial compression, Journal of Biomechanical Engineering 131, 0310061-0310066.

Ichihara, K., Taguchi, T., Sakuramoto, I., Kawano, S., Kawai, S., 2003. Mechanism of the spinal cord injury and the cervical spondylotic myelopathy: new approach based on the mechanical features of the spinal cord white and gray matter, Journal of Neurosurgery, Spine 99, 287-285.

Lai, W. M., Hou, J. S., Mow, V. C., 1991. A triphasic theory for the swelling and deformation behaviors of articular cartilage, Journal of Biomechanical Engineering 113, 245-258.

Lai, W. M., Mow, V. C., Sun, D. D., Ateshian, G. A., 2000. On the electric potentials inside a charged soft hydrated biological tissue: Streaming potential versus diffusion potential, Journal of Biomechanical Engineering 122, 336-346.

LeRoux, M. A., Setton, L. A., 2002. Experimental and biphasic FEM determinations of the material properties and hydraulic permeability of the meniscus in tension, ASME Journal of Biomechanical Engineering 124, 315-321.

Mansour, J. M., Mow, V. C., 1976. The permeability of articular cartilage under compressive strain and at high pressures, The Journal of Bone and Joint Surgery, 58, 509-516.

Perie, D., Korda, D., Iatridis, J. C., 2004. Confined compression experiments on bovine nucleus pulposus and annulus fibrosus: sensitivity of the experiment in the determination of compressive modulus and hydraulic permeability, Journal of Biomechanics 38, 2164-2171.

Quenneville, E., Binette, J. S., Garon, M., Légaré, A., Meunier, M., Buschmann, M. D., 2004. Fabrication and characterization of nonplanar microelectrode array circuits for use in arthroscopic diagnosis of cartilage diseases, IEEE Transactions on Biomedical Engineering, 51, 2164-2173.

Reynaud, B., Quinn, T. M., 2006a. Anisotropic hydraulic permeability in compressed articular cartilage, Journal of Biomechanics 39, 131-137.

Reynaud, B., Quinn, T. M., 2006b. Tensorial electrokinetics in articular cartilage, Biophysical Journal 91, 2349-2355.

Sun, D. D., Guo, X. E., Likhitpanichkul, M., Lai, W. M., Mow, V. C., 2004. The influence of the fixed negative charges on mechanical and electrical behavior of articular cartilage under unconfined compression, Journal of Biomechanical Engineering 126, 6-15.

Tadano, S., Fujisaki, K., Katoh, M., Satoh, R., 2009. Streaming potential white matter and gray matter in bovine spinal cord under compressive loading, Journal of Biomechanical Science and Engineering 4, 239-248.

Urban, J. P. G., Maroudas, A., 1979. The measurement of fixed charge density in the intervertebral disc, Biochimica et Biophysica Acta 586, 3-4.

White, A. A., Panjabi, M. M., 1978. Clinical biomechanics of the spine, J. B. Lippincott Company, Philadelphia, pp. 3-4.

Figure Captions

Fig. 1 Experimental setup for the measurement of streaming potentials under uniaxial compression conditions

Fig. 2 Cross sectional image of bovine intervertebral disc, (a) photograph of the sample and (b) locations of extraction for the compression specimens in the bovine intervertebral disc

Fig. 3 Setup of tissue specimen at the indenter

Fig. 4 Displacement profile of the uniaxial compression test and cyclic compression loading

Fig. 5 Results of compression tests in AF specimens under 0.8 mm/min compression speed (a) Compressive stress vs. compressive strain diagram (b) Streaming potential vs. compressive strain diagram of (c) Relationship between compressive stress and streaming potential.

Fig. 6 The linear coefficient k_e (mean ± S.D., n=9) in the relationship between streaming potential and stress of different parts of intervertebral tissue under uniaxial compression, AF-A: anulus fibrosus - axial; AF-C: anulus fibrosus - circumferential; AF-R: anulus fibrosus - radial directions; AN: anulus - nucleus transition area; and NP: nucleus pulposus area.

Fig. 7 Relationship between compressive stress and streaming potential under cyclic compression of at 0.01 Hz in an AF-A specimen

Fig. 8 The k_e coefficient (mean ± S.D., n=9) in the relationship between streaming potential and stress of different parts of intervertebral tissue during cyclic compression loading

Fig. 1

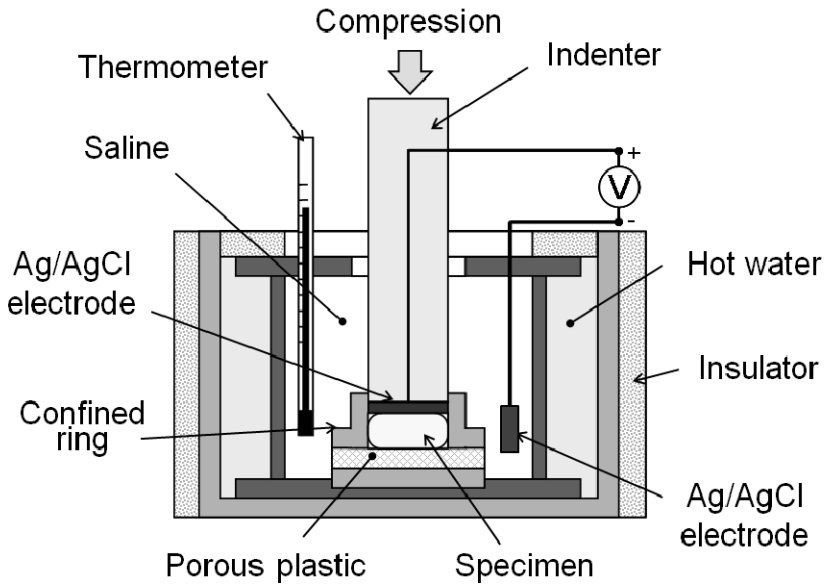
Compression
Thermometer
Indenter
Saline
+
V
-
Ag/AgCl
electrode
Hot water
Insulator
Confined
ring
Ag/AgCl
electrode
Porous plastic
Specimen

Fig. 2

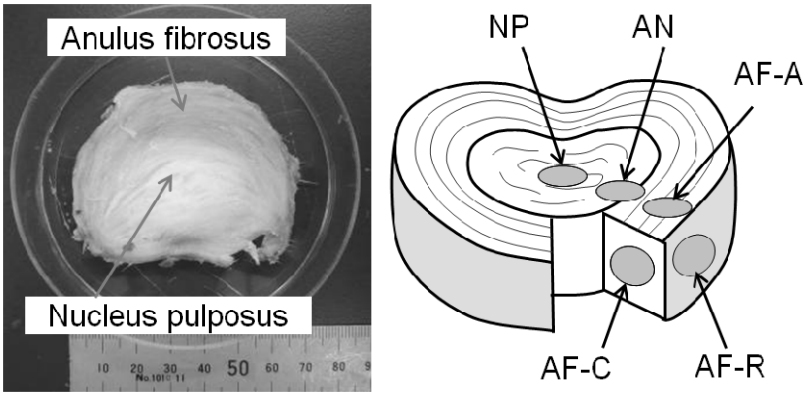

Fig. 3

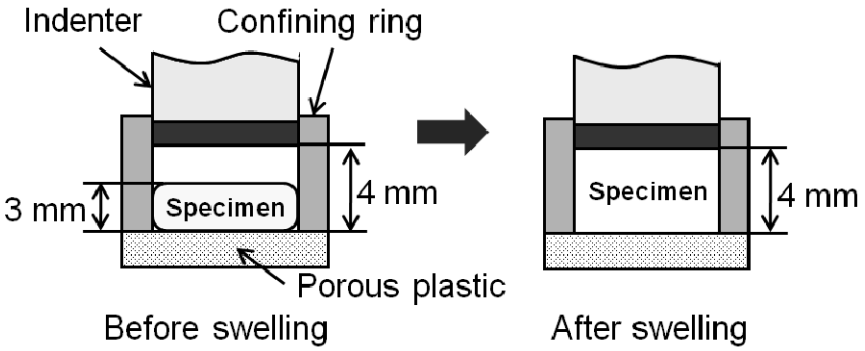
Indenter
Confining ring
3 mm
Specimen
4 mm
Porous plastic
Before swelling
Specimen
4 mm
After swelling

Fig. 4

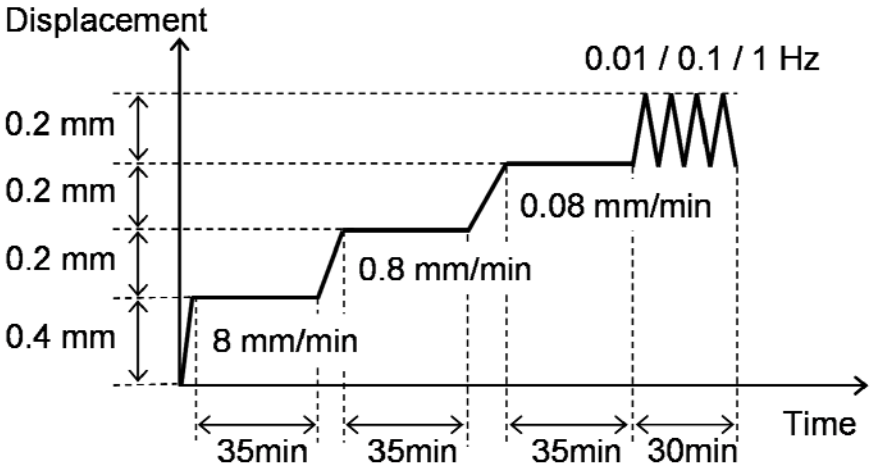
Displacement
0.01 / 0.1 / 1 Hz
0.2 mm
0.2 mm
0.2 mm
0.4 mm
0.08 mm/min
0.8 mm/min
8 mm/min
Time
35min
35min
35min
30min

Fig. 5

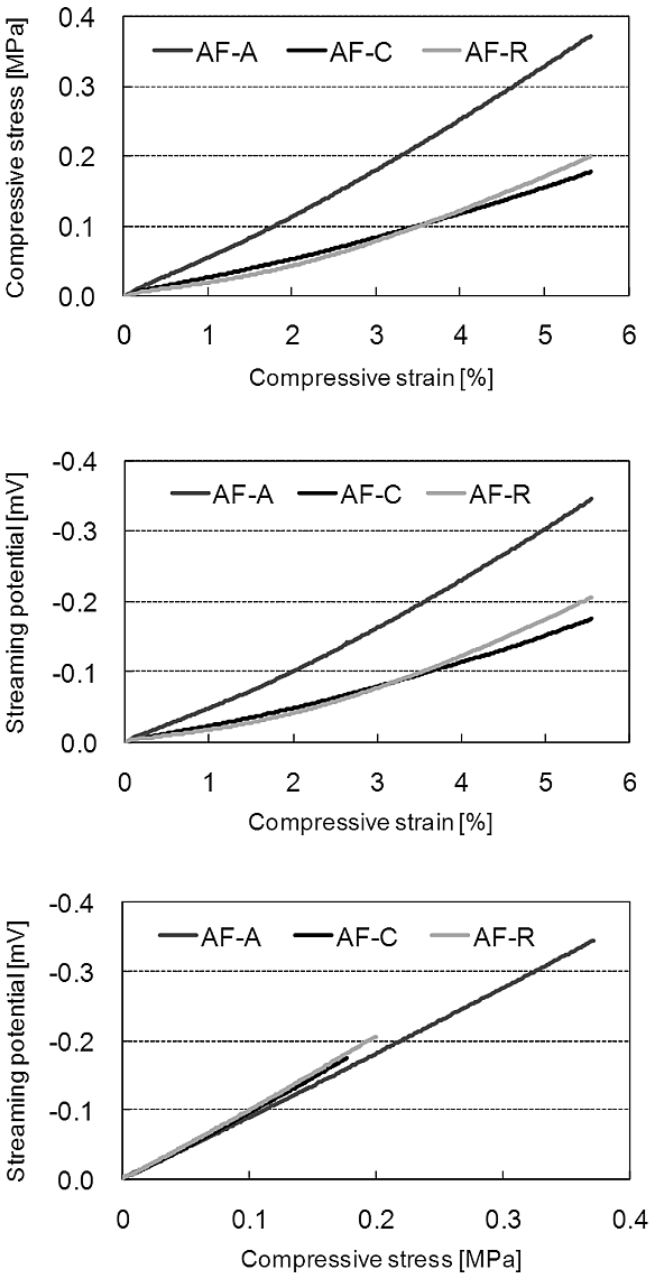
Compressive stress [MPa]
0.4
0.3
0.2
0.1
0.0
AF-A
AF-C
AF-R
0
1
2
3
4
5
6
Compressive strain [%]
Streaming potential [mV]
-0.4
-0.3
-0.2
-0.1
0.0
AF-A
AF-C
AF-R
0
1
2
3
4
5
6
Compressive strain [%]
Streaming potential [mV]
-0.4
-0.3
-0.2
-0.1
0.0
AF-A
AF-C
AF-R
0
0.1
0.2
0.3
0.4
Compressive stress [MPa]

Fig. 6

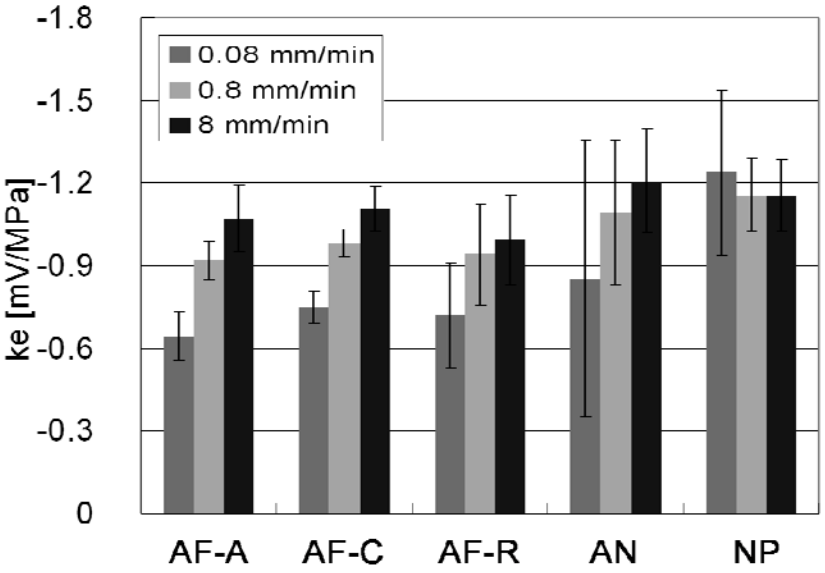
-1.8
-1.5
-1.2
-0.9
-0.6
-0.3
0
ke [mV/MPa]
0.08 mm/min
0.8 mm/min
8 mm/min
AF-A
AF-C
AF-R
AN
NP

Fig. 7

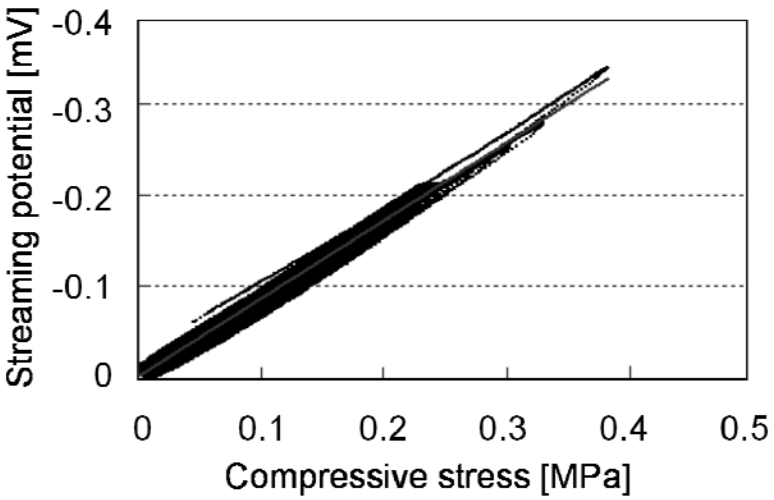
Streaming potential [mV]
-0.4
-0.3
-0.2
-0.1
0
0
0.1
0.2
0.3
0.4
0.5
Compressive stress [MPa]

Fig. 8